



Numerical analysis and geophysical monitoring for stability assessment of the Northwest tailings dam at Westwood Mine



Coulibaly Yaya, Belem Tikou, Cheng LiZhen *

Research Institute on Mines and Environment (RIME), Université du Québec en Abitibi-Temiscamingue, Rouyn-Noranda J9X 5E4, Canada

ARTICLE INFO

Article history:

Received 7 December 2016
Received in revised form 18 February 2017
Accepted 18 March 2017
Available online 26 May 2017

Keywords:

Mine tailings impoundment
Dike
Embankment
Numerical analysis
Factor of safety
Geophysical monitoring

ABSTRACT

The Westwood Mine aims to reuse the tailings storage facility #1 (TSF #1) for solid waste storage, but, downstream of the Northwest dike is considered critical in terms of stability. This paper uses numerical modeling along with geophysical monitoring for assessing the Northwest dike stability during the restoration phase. The impact of waste rock deposition in the upstream TSF #1 is considered. The geophysical monitoring is based on electrical resistivity methods and was used to investigate the internal structure of the dike embankment in different deposition stages. The numerical simulations were performed with SLOPE/W code. The results show a factor of safety well above the minimum recommended value of 1.5. Geophysical monitoring revealed a vertical variation in the electrical resistivity across the dike, which indicates a multilayer structure of the embankment. Without any current in situ data, the geophysical monitoring helped estimating the nature of the materials used and the internal structure of the embankment. These interpretations were validated by geological observation of geotechnical log of the embankment. Based on this study, it is recommended that the water polishing pond be partly filled before waste rock is deposited in TSF #1. In addition, to ensure the stability of the dike, the piezometric head monitoring prior to and during waste rock deposition is recommended.

© 2017 Published by Elsevier B.V. on behalf of China University of Mining & Technology. This is an open access article under the CC BY-NC-ND license (<http://creativecommons.org/licenses/by-nc-nd/4.0/>).

1. Introduction

The mining industry is the backbone of the economy of any natural resource country with active mines, but mining also generates large quantities of solid wastes such as tailings and waste rock that must be properly confined either in tailings storage facility (TSF) or waste rock dumps, respectively. The reason being that the exposure of these solid wastes to atmospheric conditions could result in environmental pollution by acid mine drainage or contaminated neutral drainage. When underground mining methods require that the stopes are artificially supported to allow full ore recovery, backfilling is an effective way of partial solid waste management. In a TSF, mine tailings are surrounded by the embankment dikes that must be monitored to prevent spillage of slurry tailings. However, these dikes can sometimes yield to different types of hazard and spillage of tailings pulp, which could generate extensive damage and major environmental impacts. Fig. 1 shows a break in the dam of Mount Polley (Canada) mine tailings impoundment with over 24 million m³ of tailings spilled [1]. Damage along with the death of 19 people was also reported due to the bursting of tailings

dam in Mariana, Brazil in 2015 [2]. The socioeconomic impact of disruptions in the world with the loss of life and the impact on public health increased between 2000 and 2010. About 76% of the incidents worldwide are related to upstream construction methods; 51% of incidents (breakdowns and accidents) identified by ICOLD are due to slope instability dikes following excessive stress in the foundation soil, excessive stress in the embankment of the dam and inadequate control of water pressure [3–6].

The causes of dam breakage are multiple. Apart from construction problems, poor maintenance or unusual weather is as cited by Azam and Li [7]. Other vulnerability may also be the cause of excess pore pressure accumulation due to rapid rising of the dam. Pore pressure (especially in muddy areas) will reduce the effective stresses and the shear strength of tailings [8,9]. Static and seismic liquefaction is also considered as common causes of levees particularly those enhanced by the upstream method [10,11]. As the break is a physical process (mechanical, hydraulic), in general, the breakdown for embankments occurs according to one of four classical mechanisms: external erosion, internal erosion, external instability and liquefaction [12–14]. Runoff of rain water can be the cause of the external erosion. The settlements on the crest generate cracks that promote water infiltration into the dam and this could cause internal erosion or slippage in an area

* Corresponding author.

E-mail address: Li_Zhen.Cheng@uqat.ca (L. Cheng).



Fig. 1. Illustration of tailings embankment failure-case of the Mount Polley Mine (Cariboo Regional District, Canada, 2014) [1].

of weakness. It seems relevant to the dam in this study since some settlements on the ridge have already been observed in the past (see Fig. 2).

As noted in Fig. 2, a and b are studied from Google Earth; Fig. 2c is studied by Golder Associates [18].

The Westwood Mine (owned by IAMGOLD Corp.) plans to reuse the TSF #1 for solid waste storage, but on the other side of the Northwest embankment, there is a small water polishing pond (Fig. 2). It was reported that some sporadic and localized slumps and slippage occurred on the embankment. The slippage occurs on the downstream side slope (external instability) and the upstream slope side for some reason (e.g. liquefaction of the tailings or foundation soil as a result of a probable low magnitude seismic event).

The numerical analysis has been widely used to solve complex problems of slope stability, which otherwise would not have been possible using conventional techniques [15–17]. Among other things, geophysical monitoring (electrical methods) can detect the internal cracks in the embankment. Electric resistivity of water is lower than that of rock; variations in the apparent resistivity measured by the electrical method are often correlated with the change in lithology also with the degree of water saturation in rocks (e.g. porous or fractured zones).

2. Methods and materials used

2.1. General methodologies

The aim of this study is to assess the embankment stability by the means of numerical analysis using SLOPE/W and SEEP/W codes and of geophysical methods that use Electrical resistivity [17]. The SLOPE/W code based on limit-equilibrium analysis was used to assess the embankment slope stability analysis through the calculation of the factor of safety (FS) based on the strength reduction factor (SRF) method. Before the simulation with SLOPE/W, the groundwater level (water table) that plays an important role in the stability analysis should be determined. The numerical code

SEEP/W has been used repeatedly to find the water table as a function of the variation of the water height in the upstream lake. Electrical method is widely used to detect voids, underground water, fractural zone recognition, and mineral exploration [19–43]. The distribution of water in the different layers corresponding to low resistivity values is in accordance with the high values of water content measured [44]. The difference in resistivity between the target and its surrounding materials is a key factor to ensure that this technique is viable.

2.2. FS (SLOPE/W)

In conventional methods of limit equilibrium analysis, the factor of safety (FS) is defined as the ratio between the resisting forces and the forces leading to movements [17].

$$FS = \frac{\sum S_r}{\sum S_m} \quad (1)$$

where S_r = resisting force due to friction and cohesion; and S_m = driving force tending to drag the block.

Alternatively, the FS can also be expressed as follows:

$$FS = \frac{\text{Moments resisting sliding}}{\text{Moments causing sliding}} \quad (2)$$

Amongst the most popular analytical methods of limit equilibrium analysis (see Fig. 3), is the Morgenstern-Price method, which was chosen as the analysis method (which is close to the Spencer's method), because it expresses two basic concepts for determining the FS. The FS versus lambda (Lamé coefficient) indicates the minimum FS at the point of intersection of equilibrium moment and equilibrium force. From Fig. 3, the point of intersection of the moment and the force corresponds to a FS of 2.15 per Morgenstern-Price or Spencer methods. In practice, the use of FS greater than 1.5 for static analysis of embankment stability and steady flow conditions is recommended [15,16,45].

The embankment slope stability is assessed by the effective stress analysis and the Mohr–Coulomb failure criterion was chosen:

$$\tau = c' + \sigma' \tan \phi' \quad (3)$$

where τ is the shear strength, kPa; c' the effective cohesion, kPa; ϕ' the effective internal friction angle, °; and σ' the effective normal stress, kPa, which is given as follows:

$$\sigma' = \sigma - u \quad (4)$$

where u is the pore water pressure, kPa; and σ the normal or vertical total stress, kPa.

The reduction of the effective stress σ' will reduce the shear resistance and this could promote some instabilities. For each

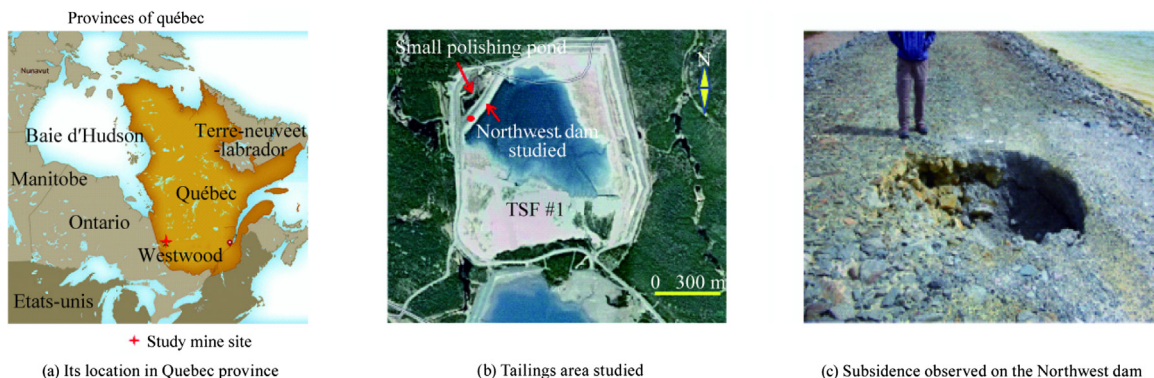


Fig. 2. Location of the Northwest dam.

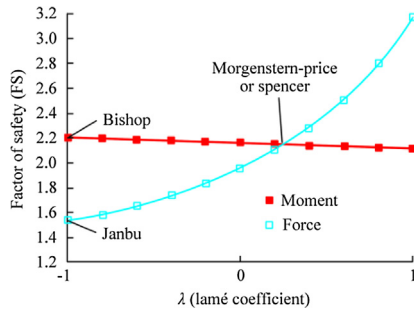


Fig. 3. Graphical plot of the FS as a function of Lamé coefficient for the moment and equilibrium forces.

simulation, the convergence of the calculations is analyzed using unbalanced forces. An unstable model is usually characterized by an non-zero value, often fluctuating; and the maximum unbalanced force and increased displacements [15]. In addition, areas of low stresses are favorable to the internal erosion [16].

2.3. Geophysical fieldwork

72 electrodes of the electrical imaging system “Syscal R1 Plus Switch 72” (IRIS instrument) were used to monitor the dam (Fig. 4). On July 14, 2015, the first pseudo-section was performed at the middle of the dam using both the Wenner-Schlumberger and Wenner configurations. The spacing between the electrodes is 5 m. The second pseudo-section is on the shelf between the water polishing pond and the Northwest dam, with 54 electrodes and the Wenner-Schlumberger and Wenner configurations, a spacing of 5 m between electrodes. The survey on July 17, 2015 made three pseudo sections using 72 electrodes; one is at a spacing of 5 m, and another at both spacing of 5 and 2.5 m, with the Wenner-Schlumberger and Wenner configurations (Fig. 4).

The pseudo-section with 5 m spacing was superimposed on that of July 14. They show a consistent result. Since the surveys on July

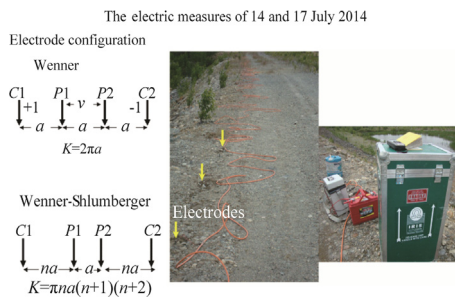


Fig. 4. Electrical measurement system used in this study.

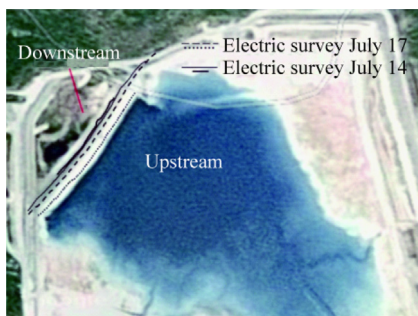


Fig. 5. Location of resistivity profiles.

14 involve the dam and the tailings, these results are presented in the interpretation section. Fig. 5 illustrates relative location of those profiles during the fieldworks.

3. Results

3.1. Numerical analysis of embankment stability (with SLOPE/W)

In general, the main objectives associated with the stability analysis of a dam are to: (1) determine the conditions of the rock mass or soil slope stability; (2) study potential failure mechanisms; (3) determine the sensitivity of slopes to different rupture trigger mechanisms, test and compare the different support options and stabilization; and (4) design slopes optimally for safety and cost saving. The purpose of the numerical modeling is to determine the FS, in a perspective of assessing slope stability of the Northwest embankment, using SEEP/W and SLOPE/W.

By convention, the design of dam geometry would ensure a minimum FS of 1.4–1.5 for each phase of construction. The minimum FS of 1.5 was also used in the dam stability analysis in Sweden by and the same value is recommended by the Canadian Dam Association for the long-term analysis [16,46]. It was noticed that the values of the FS prescribed in the “Guide and how to prepare for the restoration of mining sites in Quebec” by the Québec Ministry of Energy and Natural Resources, are also between 1.3 and 1.5 [45].

3.1.1. Geometry of the dam

According to observations in issue, the slope of the Northwest dam varies between 26.6° (upstream side) to 33.7° (downstream side). It reaches 15 m high. For numerical simulations, it is the geometry of the dam at the end of the construction that will be reproduced. The succession, the thickness, and extent of the layers in this initial model are shown in Fig. 6. The lower limit in depth would be the very dense moraine layer overly on the bedrock. These two layers are not included in the numerical models of stability analysis because they can be already considered as stable and remain in balance even after the construction of the dam.

3.1.2. Estimation of material properties

The parameter values used in SLOPE/W (Table 1) mainly come from a private geotechnical report for the mining company. The

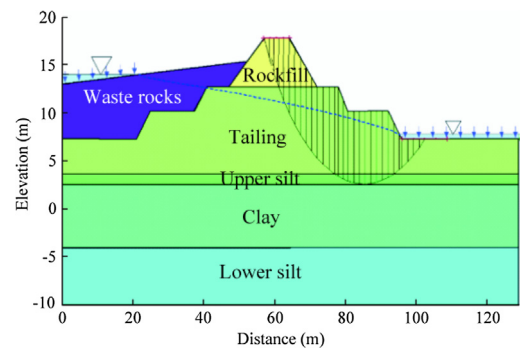


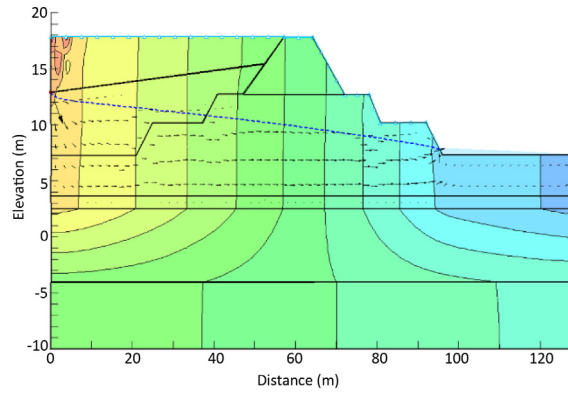
Fig. 6. Geometry of the Northwest dam (using data from [47]).

Table 1
Parameters values used in modeling.

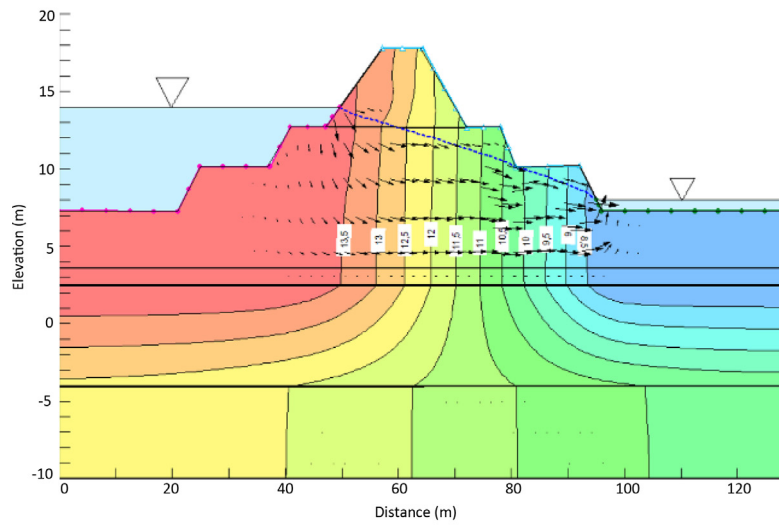
Layer	γ (kN/m ³)	ϕ' (°)	C' (kPa)	τ (kPa)
Tailing	19.0	35	0	0
Silt	19.2	28	0	0
Silty clay	16.5	30	0	40
Rockfill	19.5	38	0	38
Waste rock	18.1	38	0	0

Table 2
Reference of saturated hydraulic conductivity values (k_h ; k_v).

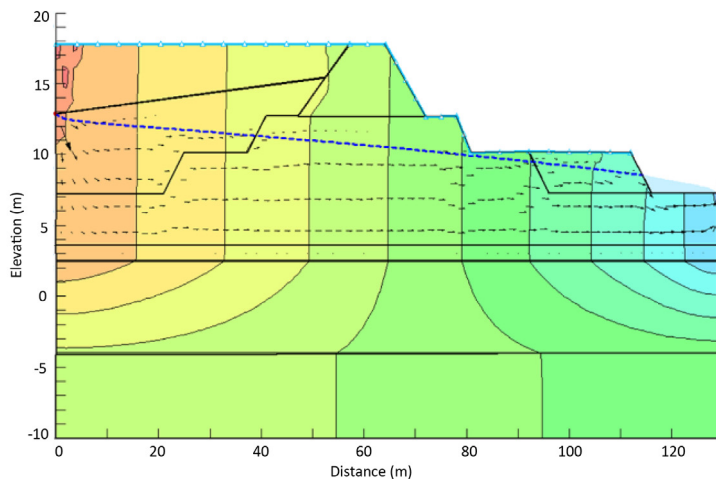
Ref.	Parameter	Rockfill	Tailing	Silt	Silt clay
Ormann et al. [16]	k_h (cm/s)	10^{-3}	10^{-8}		10^{-9}
	k_v (cm/s)	10^{-3}	10^{-9}		10^{-9}
Tanriseven [51]	k_h (cm/s)	10^{-6}	10^{-6} – 10^{-7}	10^{-7}	10^{-9}
	k_v (cm/s)	10^{-6}	10^{-7} – 10^{-8}	10^{-8}	10^{-9}
Mbonimpa et al. [50]	k_v (cm/s)			10^{-8}	10^{-6} – 10^{-11}
Chapuis and Aubertin [49]	k_v (cm/s)			10^{-8}	10^{-9}
Values used in SEEP/W	$k_h = k_v$ (cm/s)	10^{-6}	10^{-7}	10^{-8}	10^{-9}



(a) WT level due to precipitation, w/o rockfill



(b) Iso-values of hydraulic head in relation to the water table



(c) WT level due to precipitation, with rockfill

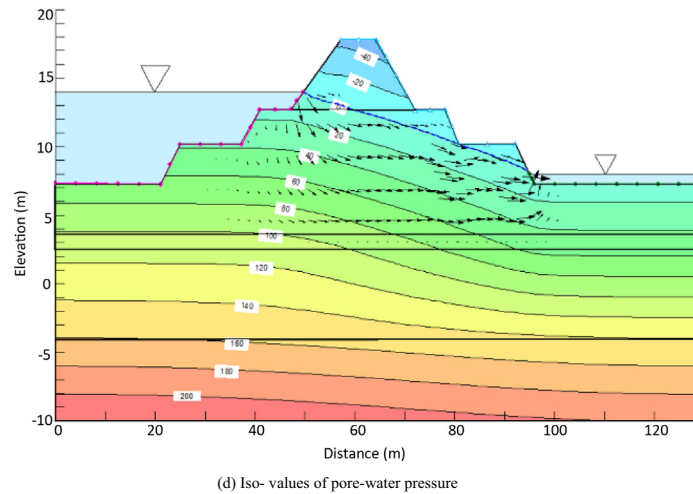


Fig. 7. Water table level estimation with varying factors.

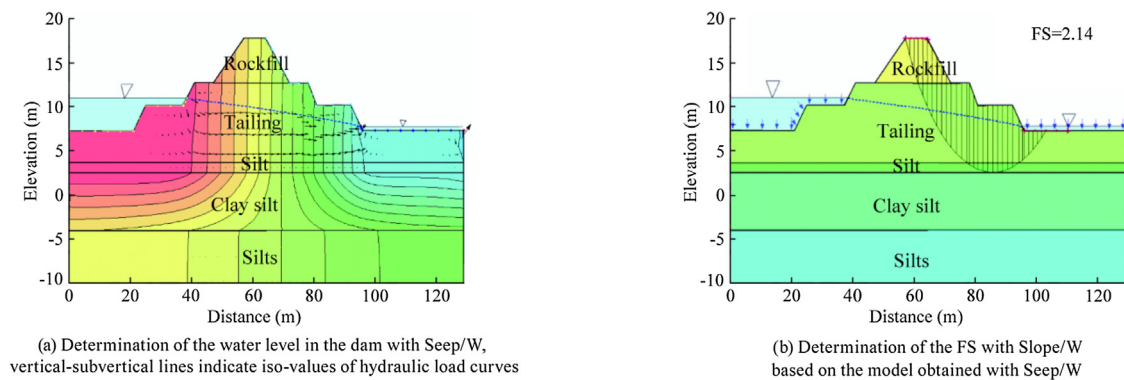


Fig. 8. Illustration of stability analysis.

value of the unit weight of the rockfill is estimated based on previous works on similar situation as for example, a value of 19 kN/m^3 from and 20 kN/m^3 [10,48]. Therefore, the average value of 19.5 kN/m^3 is used in the present study.

3.1.3. Determination of the level of the water table

The numerical code SEEP/W has been used repeatedly to find the water table as a function of the variation of the water column in the upstream lake. The saturated hydraulic conductivity values (Table 2) were collected from the literature [16,49–51]. The Mine's report also shows a vertical hydraulic conductivity estimated in the range of $5 \times 10^{-8} \text{ cm/s}$ for the silty clay and between 5×10^{-3} and $5 \times 10^{-6} \text{ cm/s}$ for silts.

In this study, the volumetric water content was estimated to be 0.5 for each of the materials, since it's known that the dam is not entirely saturated (above the water table).

Therefore, the same geometry as the initial model was used for varying the level of water in the upstream lake while filling it with waste rock in the simulation. The boundary conditions are set to zero pressure at the downstream end of the dam in SEEP/W. An average value of 2.10^{-8} m/s is used for potential infiltration in the dam. This value was estimated from the rainfall data of Mont-Brun station (Rouyn-Noranda) according to the Institute of Statistics of Québec [52]. Fig. 7 illustrates the water table (WT) level due to the precipitation only, without rockfill layer in the downstream lake (Fig. 7a), the iso-values of hydraulic head relative to the water table (Fig. 7b), the water table level due to the precipitation only, with a rockfill layer in the downstream lake (Fig. 7c), the iso-values of pore-water pressure (Fig. 7d).

Once basic parameters are set up, using Morgenstern-Price analysis method and Mohr–Coulomb failure criterion; defining the specific gravity for each material, the effective cohesion, and the effective angle of internal friction, then the analysis is run for the calculation of a minimum FS (e.g. $\text{FS} = 2.14$ in Fig. 8).

3.1.4. Factor of security in situ condition

The input parameters for each type of material are: unit weight (γ), effective cohesion (c') and effective internal angle of friction ϕ' , after determining the water level in the structure, FS of 2.0 is obtained. Fig. 9 shows the result of the analysis that indicates FS value of 2.0 which is higher than the recommended value of

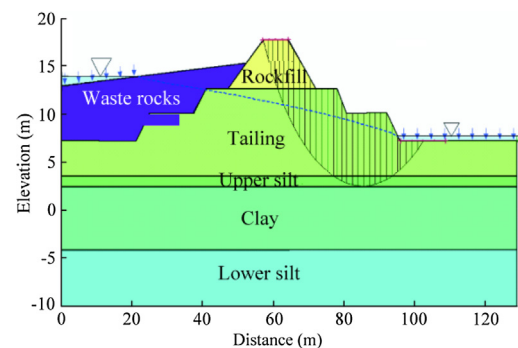


Fig. 9. Stability analysis of the embankment slope showing FS of 2.0 at the start of the tailings impoundment filling.

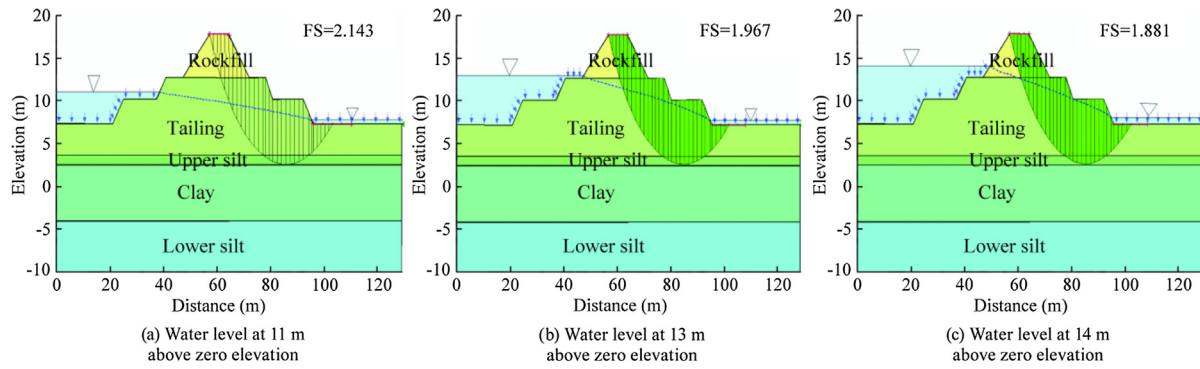


Fig. 10. Stability analysis for different water levels.

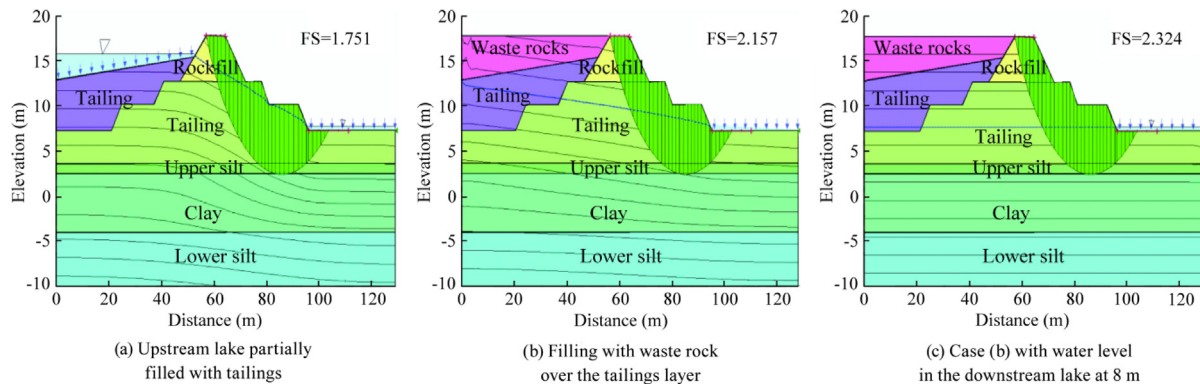


Fig. 11. Stability analysis for different upstream lake filling conditions.

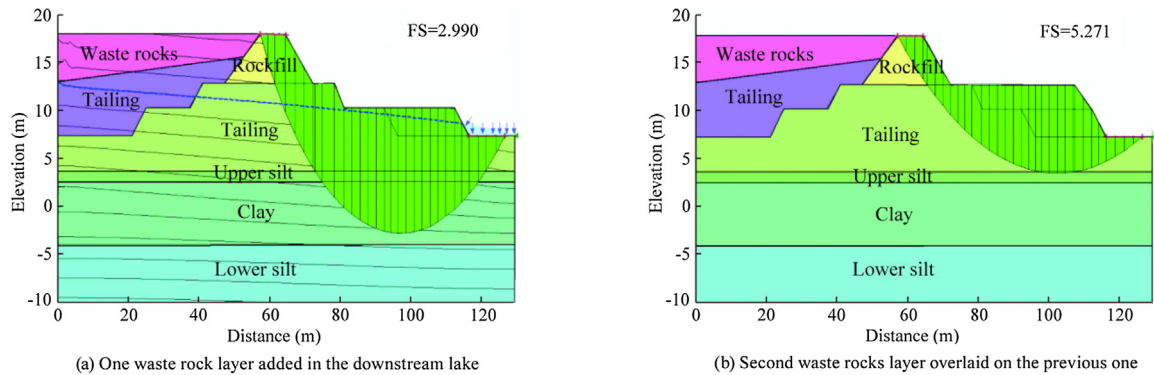


Fig. 12. Stability analysis considering downstream lake filling process.

FS = 1.5. This value corresponds to the start of the tailings impoundment filling which is the current state of the embankment. This result shows that the embankment is currently stable.

3.1.5. Influence of the water level on the upstream side of the dam

Fig. 10 shows that when the water level rises in the upstream lake, the minimum FS decreases. There is no storage of materials and also considering that the depth of water in the downstream lake is fixed. When the water level (upstream side) is 11 m to zero elevation, the FS is 2.14 (Fig. 10a). When the water level reaches almost 13 m, the FS decreases to 1.97 (Fig. 10b) while at 14 m of water level the FS is only 1.88 (Fig. 10c).

3.1.6. Effect of filling the upstream lake of the dam

In a more realistic case where the tailings in the upstream lake form a slightly inclined layer, the FS increases compared to the case where the lake contains only water (Fig. 11a). When more fills in

the upstream lake with waste rock, assuming there is only water infiltration from rainfall, the FS goes from 1.75 to 2.16 (Fig. 11b). If the water level in the downstream lake rises to 8 m and then in stationary regime, there is an even higher FS of 2.32 (Fig. 11c) for the dike.

By filling part of the downstream lake with waste rock and the infiltration conditions of potential water either side of the dam, the FS is 2.99 (Fig. 12a). Adding another layer of waste rock over the existing one in downstream side and under the same conditions where there is only the infiltration of water from rainfall on either side of the dam, the FS increases significantly to 5.27 (Fig. 12b) as that is expected.

3.1.7. Influence of cohesion and angle of friction on FS

To determine the effects of the change in cohesion and the angle of friction of fill layers (rockfill and tailings), several simulations were performed and the values the FS are shown in Table 3. One

Table 3

FS when cohesion and angle of friction of rockfill and tailings layers are varied independently.

Cohesion (kPa)	Angle of friction (°)	Unit weight (kN/m ³)	FS
<i>(a) Rockfill</i>			
0	20	18.1	1.856
0	42	18.1	1.964
0	60	18.1	2.072
0	42	18.1	1.964
10	42	18.1	2.013
20	42	18.1	2.064
0	42	18.1	1.964
0	42	23.1	1.848
0	42	24.3	1.824
0	42	30.0	1.729
0	12	19	0.755
0	35	19	1.964
0	53	19	2.582
<i>(b) Tailings</i>			
0	35	19	1.964
10	35	19	2.222
20	35	19	2.391
0	35	12	1.28
0	35	19	1.964
0	35	25	2.349

can observe that there would be the embankment failure when the tailings effective cohesion c' is zero and the effective internal angle of friction is 12° (FS = 0.755). Also, when the tailings effective cohesion is zero with an angle of friction of 35° and a unit weight of 12 kN/m³, the FS = 1.28 (which is lower than the recommended value of 1.5).

It should however be noted that these two scenarios are unlikely because the tailings effective angle of friction would be close to 30° while it is very unlikely that the tailings can have a unit

weight lower than 14 kN/m³ (specific gravity of 2.67 and slurry solid mass content of 50%).

Data in Table 3 are used to construct different graphs that are presented in Figs. 13–15 and illustrating the influence of the effective cohesion and internal angle of friction on the FS. Figs. 13–15 show that the effective cohesion and angle of friction, which are the shear strength parameters shown in Eq. (3), have a direct influence on the FS. In fact, FS increases with the increase of the cohesion and the angle of friction. For a similar range of variation of c' and ϕ' the trend of the FS is more pronounced for the tailings than for the rockfill (Fig. 15).

3.2. Resistivity tomography using RES2DINV software

The resistivity data is processed by the RES2DINV inversion software (GEOTOMO Software). It estimates apparent resistivity values for each rectangular block of the subsurface by fitting the observation based on the least-square principal. The software determines the error criterion, the inverted resistivity model is then modified to reduce the degree of error between the apparent resistivity measured and calculated. The inversion operation is repeated iteratively until the error reaches to tolerant value [53]. As a layered structure was preliminary interpreted from georadar survey on the dike, the default smoothness-constrained inversion method is used for the electric resistivity data inversion [54]. By comparing the inversion result of the pseudo-section in the middle of the dam (Fig. 16a) with that on the shelf (Fig. 16b), they show consistent structure with the observation in a geotechnical drilling F-95-1 [47]. According to geotechnical logs, from surface to the end of drilling the dam consists of rockfill, tailings slits, the silty clays, the silt and moraine layer. An outcrop was observed at the North-east end of the dam. This outcrop corresponds to schistose sandstone; its resistivity value was estimated between 100 and

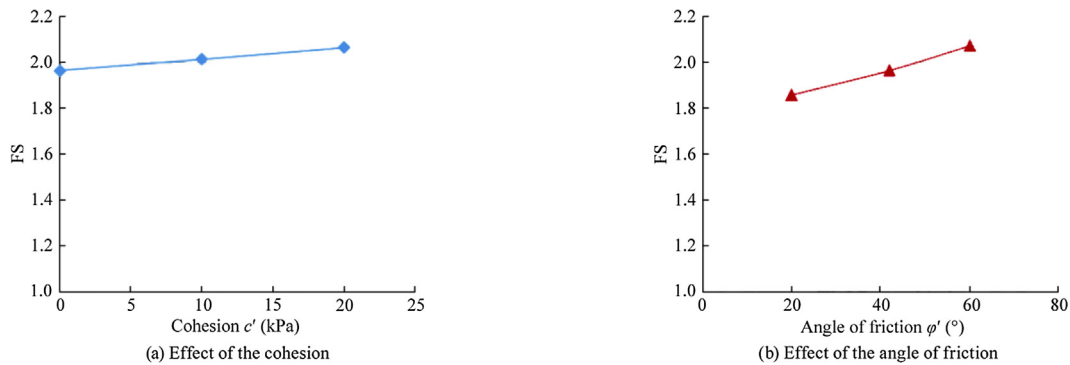


Fig. 13. Variation in FS as a function of cohesion and angle of friction for the rockfill material.

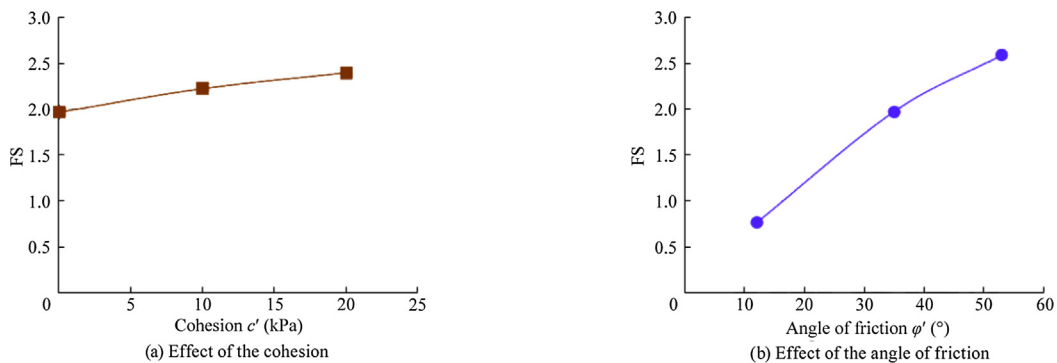


Fig. 14. Variation in FS as a function of the cohesion and angle of friction for the tailings.

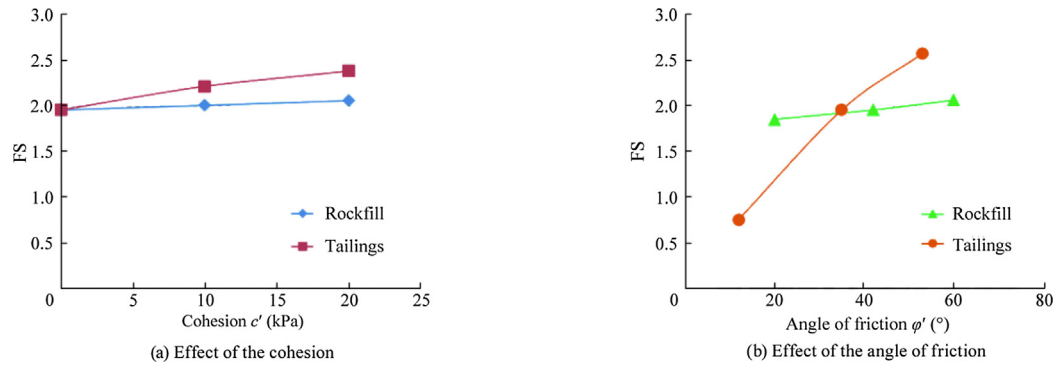


Fig. 15. Variation in the FS as a function of the cohesion and angle of friction for the tailings and rockfill.

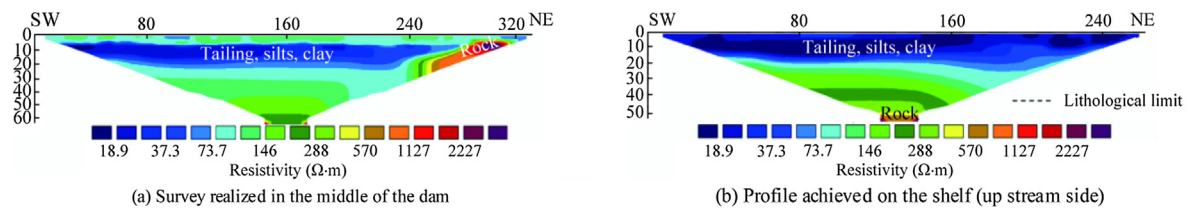


Fig. 16. RES2DINV inversion results.

Table 4

Comparison the stratigraphic profile of geotechnical drilling and lithology estimated with the resistivity interpretation.

Item	Geotechnical drilling F-95-1	Electric resistivity
Rockfill	0–5 m	73–300 (Ω m) (0–5 m)
Tailings	5–14 m	18–73 (Ω m)
Silty clay	14–20 m	(5–27 m)
Silt	20–27 m	
Moraine layer	>27 m	73–500 (Ω m) (27–50 m)
Bedrock		>570 (Ω m) (>65 m)

1000 Ω m [55]. The inversion results show that there is a resistivity contrast between different materials; however, it is difficult to distinguish the tailings silts and silty clays from the resistivity. With the help of drilling data, we interpret the distribution of the electrical resistivity in term of changes in materials as cited in Table 4.

Taking into account the variation of water content which affects the electrical resistivity, it is sometimes difficult to interpret lithologic boundaries according to the 2D model of the resistivity inversion. A greater electrical conductivity could be due to high water content as shown by Maqoud et al., where low resistivity values are coincide with high values of measured water content [44]. Based on the amended soil and rock, resistivity values from the internal structure of the dam are interpreted as follow [56]:

- (1) The rockfill at the surface is highly heterogeneous in grain size also in water content. Probably this explains the large range of the resistivity variations from 73 up to 300 Ω m. The thickness of this layer is less than 5 m.
- (2) As the shelf is covered by tailings that are comprised of very fine particles and water-saturated, the inversion result (Fig. 16b) shows this top layer a low resistivity less than 73.5 Ω m. The comparison between this inversion result with that in the middle of the dam (Fig. 16a), the low resistivity (<100 Ω m) layer between 5 and 25 m is interpreted as the tailings and silty clay layer (Fig. 16).

- (3) Since the geotechnical drilling stopped at 27.5 m, from an outcrop next to the Northeast end of the dam it is believed that the bedrock may have the same composition as the outcrop. The resistivity of the outcrop is more than 500 Ω m (Fig. 16a), the bedrock could be at more than 50 m of the depth (Fig. 16b). Therefore, the moraine between the tailings/silty clay layer and bedrock is about 20 m in the thickness.

4. Conclusions

In this paper, the stability analysis for the Westwood Mine tailings embankment and geophysical monitoring results are presented. The calculated values of the FS are higher than 1.5, which meets the standard recommendations set by the Quebec Ministry of Natural Resources and Wildlife for static loading and steady flow conditions. In all cases of realistic geometric representation of the embankment, the minimum FS is greater than 1.5, thus confirming the stability of the embankment studied. The performed electrical tomography shows that it is possible to distinguish the different structures of the Northwest embankment of Westwood Mine tailings storage facility without employing a destructive method. The geophysical technique has identified the internal structure of the dam which is consistent with the observed lithology in geotechnical drilling F-95-1.

The method of electrical resistivity demonstrates some heterogeneity of the materials of the dam, particularly in the upper layer of riprap by a strong variation of resistivity, probably caused by the variation in particle size of materials. Such heterogeneity could potentially cause differential settlement of the dam in time. The saturated zone in water as the layer of tailings is characterized by low electrical resistivity values (<100 Ω m). This study demonstrates the great potential of geophysical methods for monitoring embankments.

By combining the study of the internal structure and stability analyses, the results will be useful not only for the present condition assessment of the dam, but also for planning new developments. An analysis of deformation and effective stress would be

useful in future work. If the effective stress decreases, the shear strength of the material decreases and this may generate rupture. Whenever possible, it would be good to carry out geotechnical drilling to collect samples in order to determine real geomechanical parameters and update the stability analysis.

Acknowledgement

This research was financially supported by NSERC (Natural Sciences and Engineering Research Council of Canada) Engage grants. The authors would like to acknowledge NSERC for this support. The authors also wish to thank industry partner, IAMGOLD Corporation (Westwood Mine), including the Superintendent of Environment Department, Mr. Sylvain Lortie for their collaboration in this project. We would also like to thank Pierre-Luc Dallaire and Simon Nadeau for his participation in field work and technical assistance.

References

- [1] Simeon A, Lapointe U. Mount polley pine disaster's first anniversary no reason to celebrate. *Georgia Straight*: Vancouver Free Press Publishing Corp; 2015.
- [2] Kiernan P. Engineers say Brazilian disaster shows world-wide danger from Hoover Dam-size earthen structures holding tailings waste. *The Wall Street J* 2016. Updated April 5.
- [3] Rico M, Benito G, Salgueiro AR, Díez-Herrero A, Pereira HG. Reported tailings dam failures: A review of the European incidents in the worldwide context. *J Hazard Mater* 2007;152(2):846–52.
- [4] ICOLD (international commission on large dams), bulletin 104. Monitoring of tailings dams, review and recommendations; 1996.
- [5] ICOLD Bulletin 121. Tailings dams, risk of dangerous occurrences, lessons learnt from practical experiences; 2001.
- [6] Mbonimpa M. Géotechnique minière. Notes de cours: Université du Québec en Abitibi-Témiscamingue (UQAT); 2014.
- [7] Azam S, Li Q. Tailings dam failures: a review of the last one hundred years. *Geotechnical News Magazine*, December 2010.
- [8] Engels J, Schönhardt M, Witt KJ, Benkovic I, Berta Z, Csóvári M, Georgescu DP, Radulescu CA, Zlagnean, M Böhm J, Debreczeni Á, Gombkötő I, Koffa E, Mylona E, Paspaliaris I, Xenidis A. Tailings management facilities-intervention actions for risk reduction. *European Research and Technological Development Project Report*; 2004. 52 p.
- [9] Zardari MA. Stability of tailings dams: focus on numerical modelling. Licentiate thesis, Luleå University of Technology; 2011. 13 p.
- [10] Ormann L, Zardari MA, Mattsson H, Bjelkevik A, Knutsson S. Numerical analysis of strengthening by rockfill embankments on an upstream tailings dam. *Can Geotech J* 2013;50(4):391–9.
- [11] Zardari MA, Ormann L, Mattsson H, Knutsson S. Numerical analysis of staged construction of an upstream tailings dam. In: *Proceedings of national conference on civil engineering*, 28/04/2014-29/04/2014, department of civil engineering, Quest Nawabshah, Pakistan; 2014. p. 150–60.
- [12] Mériaux P, Royet P, Folton C. Surveillance, entretien et diagnostic des digues de protection contre les inondations: Guide pratique à l'usage des propriétaires et des gestionnaires. Cemagref Editions; 2004. 181 p.
- [13] Lepetit L. Etude d'une méthode de diagnostic des digues avec prise en compte du risque de liquéfaction. Auvergne: Université Blaise Pascal - Clermont 2; 2002.
- [14] Serre D. Evaluation de la performance des digues de protection contre les inondations - Modélisation de critères de décision dans un Système d'Information Géographique. Université de Marne-La-Vallée; 2005.
- [15] Eberhardt E. Rock slope stability analysis-utilization of advanced numerical techniques. Département of Earth and Ocean Sciences at UBC Report. University of British Columbia (UBC), Vancouver, Canada. 41 p.
- [16] Ormann L, Zardari MA, Mattsson H, Bjelkevik A, Knutsson S. Numerical analysis of strengthening by rockfill embankments on an upstream tailings dam. *Can Geotech J* 2013;50(5):391–9.
- [17] GeoSlope International Ltd. SEEP/W Users Guide. GeoSlope International, Calgary, Canada; 2007.
- [18] Golder Associates. Réalisation de tranchée d'exploration digue nord-ouest du parc 1, mine doyon; 2004.
- [19] Denahan BJ, Smith DL. Electrical resistivity investigation of potential cavities underlying a proposed ash disposal area. *Environ Geol Water Sci* 1984;6(1):45–9.
- [20] Maillol JM, Seguin MK, Gupta OP, Akhauri HM, Sen N. Electrical resistivity tomography survey for delineating uncharted mine galleries in West Bengal, India. *Geophys Prospect* 1999;47(2):103–16.
- [21] Ernstson K, Kirsch R. *Geoelectrical methods*. Berlin: Springer; 2006.
- [22] Pánek T, Margielewski W, Táborik P, Urban J, Hradecký J, Szura C. Gravitationally induced caves and other discontinuities detected by 2D electrical resistivity tomography: case studies from the Polish Flysch Carpathians. *Geomorphology* 2010;123(1–2):165–80.
- [23] Martínez-Pagán PD, Gómez-Ortiz T, Martín-Crespo JJ, Rosique M. The electrical resistivity tomography method in the detection of shallow mining cavities. A case study on the Victoria Cave, Cartagena (SE Spain). *Eng Geol* 2013;156(9):1–10.
- [24] Olayinka AI, Sogbetum AO. Laboratory measurement of the electrical resistivity of some Nigerian crystalline basement complex rocks. *African J Sci Technol* 2002;3(1):93–7.
- [25] Knight RJ, Enders AL. An introduction to rock physics principles for near-surface geophysics. In: *Near-surface geophysics*. Society of exploration geophysicists; 2005. p. 31–70.
- [26] Samouëlian A, Cousin I, Tabbagh A, Bruand A, Richard G. Electrical resistivity in soil science: a review. *Soil Tillage Res* 2005;83(2):173–93.
- [27] Slater L. Near surface electrical characterization of hydraulic conductivity: from petrophysical properties to aquifer geometries—a review. *Surv Geophys* 2007;28(2–3):169–97.
- [28] Kazakis N, Vargemelis G, Voudouris KS. Estimation of hydraulic parameters in a complex porous aquifer system using geoelectrical methods. *Sci Total Environ* 2016;550:742–50.
- [29] Aina A, Olorunfemi MO, Ojo JS. An integration of aeromagnetic and electrical resistivity methods in dam site investigation. *Geophysics* 1996; 61(2):349–56.
- [30] Johansson S. *Seepage monitoring in embankment dams*. Stockholm: Royal Institute of Technology de Stockholm; 1997.
- [31] Panthulu TV, Krishnaiah C, Shirke JM. Detection of seepage paths in earth dams using self-potential and electrical resistivity methods. *Eng Geol* 2001;59(3–4):281–95.
- [32] Jackson PD, Northmore KJ, Meldrum PI, Gunn DA, Hallam JR, Wambura J, et al. Non-invasive moisture monitoring within an earth embankment - a precursor to failure. *NDT and E Int* 2002;35(2):107–15.
- [33] Fauchard C, Mériaux P. *Méthodes géophysiques et géotechniques pour le diagnostic des digues de protection contre les crues*. Cemagref Editions; 2004. 124 p.
- [34] Hennig T, Weller A, Canh T. The effect of dike geometry on different resistivity configurations. *J Appl Geophys* 2005;57(4):278–92.
- [35] Mainali G. *Monitoring of tailings dams with geophysical methods*. Sweden: Lulea University of Technology; 2006.
- [36] Cho IK, Yeom JY. Crossline resistivity tomography for the delineation of anomalous seepage pathways an embankment dam. *Geophysics* 2007;72(2):G31–8.
- [37] Fargier Y. Développement de l'Imagerie de Résistivité électrique pour la reconnaissance et la surveillance des ouvrages hydrauliques en terre. Nantes: École Centrale de Nantes; 2011.
- [38] Sjö Dahl P, Dahlin T, Zhou B. 2.5D resistivity modeling of embankment dams to assess influence from geometry and material properties. *Geophysics* 2006;71(3):G107–14.
- [39] Sjö Dahl P, Dahlin T, Johansson S, Loke MH. Resistivity monitoring for leakage and internal erosion detection at Hällby embankment dam. *J Appl Geophys* 2008;65(3–4):155–64.
- [40] Sjö Dahl P, Dahlin T, Johansson S. Using the resistivity method for leakage detection in a blind test at the Rassvatn embankment dam test facility in Norway. *Bull Eng Geol Env* 2010;69(4):643–58.
- [41] Kuras O, Pritchard JD, Meldrum PI, Chambers JE, Wilkinson PB, Ogilvy RD, et al. Monitoring hydraulic processes with automated time-lapse electrical resistivity tomography. *CR Geosci* 2009;341(10–11):868–85.
- [42] Daniels JJ, Dyck AV. Borehole resistivity and electromagnetic methods applied to mineral exploration. *IEEE Trans Geosci Remote Sens* 1984;GE-22(1):80–7.
- [43] Douglas WO, Yaoguo L, Colin G, Peter K, Theo A, Alan K, et al. Applications of geophysical inversions in mineral exploration; 1998.
- [44] Maqsoud A, Bussièrre B, Aubertin M, Chouteau M, Mbonimpa M. Field investigation of a suction barrier designed to control oxygen barrier slope-induced desaturation. *Can Geotech J* 2011;48(1):53–71.
- [45] Ministère des ressources naturelles et de la faune Guide et modalités de préparation du plan et exigences générales en matière de restauration des sites miniers au Québec; 1997.
- [46] Canadian Dam Association – ACB, 2013, Dam safety guidelines 2007 (édition 2013). 82p.
- [47] Golder associates. Closure plan report and restoration of Doyon Mine; 1999.
- [48] Massiéra M, Vautour J, Coulibaly Y, Hammamji Y, Szostak-Chrzanowski A. Comportement des barrages en enrochement avec masque amont en béton de ciment fondés sur des alluvions granulaires. In: *Proceedings of the 2006 annual general conference of the Canadian society for civil engineering*. Calgary, Alberta, Canada, May 23–26; 2006.
- [49] Chapuis RP, Aubertin M. A simplified method to estimate saturated and unsaturated seepage through dikes under steady state conditions. *Can Geotech J* 2001;38(6):1321–8.
- [50] Mbonimpa M, Aubertin M, Chapuis RP, Bussièrre B. Practical pedotransfer functions for estimating the saturated hydraulic conductivity. *Geotech Geol Eng* 2002;20(3):235–59.
- [51] Tanriseven EN. Stability investigation of ETI copper mine tailings dam using finite element analysis. Ankara: Middle East Technical University; 2012.
- [52] Institut de la statistique du Québec. Ministère du Développement durable, de l'Environnement, de la Faune et des Parcs, Normales climatiques 2014; 1981–2010.
- [53] Boussicault B. Étude géophysique d'une digue de rétention d'eau, parc à résidus miniers solbec, stratford, Québec. Mémoire de Maître en Sciences de la Terre. Université du Québec, INRS Eau Terre et Environnement, Canada; 2007.

- [54] Coulibaly Y. Monitoring de la digue nord-ouest du parc à résidus miniers n°1 de doyon dans une perspective d'évaluation de la stabilité pendant la phase de restauration. Institut de recherche en mines et environnement (IRME), Université du Québec en Abitibi-Témiscamingue et Polytechnique Montréal, Canada; 2016.
- [55] Savoie A, Trudel P, Sauvé P, Hoy L, Kheang L. Géologie de la mine Doyon (région de Cadillac). Ministère de l'Énergie et des Ressources du Québec 1991:80. ET-90-05.
- [56] Palacky GJ. Resistivity characteristics of geologic. *Electromagnetic methods in applied geophysics theory*. Soc Exploration Geophys 1987;1:53–129.